



## MODELING, SIMULATION AND STABILITY ANALYSIS USING MATLAB OF A HYBRID SYSTEM SOLAR PANEL AND WIND TURBINE IN THE LOCALITY OF PUNTAHACIENDA-QUINGEO IN ECUADOR

 D. Icaza<sup>1</sup>

 S. Sami<sup>2+</sup>

<sup>1,2</sup>Catholic University of Cuenca, Cuenca, Ecuador

<sup>2</sup>Email: [dr.ssami@transpacenergy.com](mailto:dr.ssami@transpacenergy.com)



(+ Corresponding author)

### ABSTRACT

#### Article History

Received: 19 January 2018

Revised: 15 February 2018

Accepted: 19 February 2018

Published: 21 February 2018

#### Keywords

Hybrid system  
Solar PV  
Wind turbine  
Modeling  
Simulation  
Stability analysis  
MATLAB  
Experimental validation.

The modeling, simulation and analysis of the energy conversion equations describing the behavior of a hybrid system PV and wind turbine, and hybrid system for electrical power generation are presented. A numerical model based on the aforementioned equations was developed, coded and results were presented, discussed compared to experimental data reported in the literature. The model is intended for optimization and as design tool for such hybrid systems. The model predicted results compared fairly to experimental data under various conditions. A stability analysis was also performed by the mathematical modeling for the hybrid system. It is important to point out that this analysis has been carried out so that in the near future one of these power generation systems to be exploited to a great extent in the locality of Quingeo-Puntahacienda.

**Contribution/Originality:** This study contributes to the optimization of hybrid systems PV-Wind and that can be used as design tool for hybrid systems intended for implementation in remote zones without access to the grid. It is important to point out that this study has been carried out so that in the near future remote areas localities such as Quingeo-Puntahacienda can benefit from renewable energy technologies.

### 1. INTRODUCTION

Renewable and non-conventional energy generation methods such as wind, solar, hydropower, biomass, geothermal, thermal storage and waste heat recovery solutions for remote areas of Quingeo such as the localities surrounding Puntahacienda in Ecuador are not directly accessible by the electrical grid. A hybrid system is an integrated system of two or more renewable energy systems, and can complement each other, provides a higher quality and reliable power source independent of the utility's grid network (Garcia, 2006; Department of Energy, 2007; Kavitha and Kamdi, 2013; Zhang *et al.*, 2013; Binayak *et al.*, 2014; Neira and Velecela, 2014; Peterseim *et al.*, 2014; Srinivas and Reddy, 2014; Iftekhar *et al.*, 2015; Sami and Icaza, 2015; Sami and Icaza, 2015; Sami and Marin, 2017). Wind turbine and PV, has become increasingly an attractive option, compared to cost of fossil fuels, land developments and thermal technology (Garcia, 2006; Department of Energy, 2007; Kavitha and Kamdi, 2013; Binayak *et al.*, 2014; Srinivas and Reddy, 2014; Iftekhar *et al.*, 2015; Sami and Icaza, 2015; Sami and Icaza, 2015; Sami and Marin, 2017).

Neira and Velecela (2014) presented and discussed the electrification of the rural area and a review of the autonomous system of power such as; Solar and wind. In addition, references (Kavitha and Kamdi, 2013) and (Deissler, 1964; Howell *et al.*, 1982; Covarrubias *et al.*, 2005; Wenham, 2007; Atideh and Zhenhua, 2008; Fargali *et al.*, 2010; Craig and Zhiwen, 2011; Marreno, 2011; Penyarat and Pascal, 2012; Akikur *et al.*, 2013; Mustafa, 2013; Saha *et al.*, 2013; Castillo *et al.*, 2014; Dustin and Jack, 2014; Yoshimasa *et al.*, 2015) presented and analyzed the feasibility and importance of the use of wind energy in global electrification. Reference (Sami and Icaza, 2015) analyzed and compared a simulation model of the proposed system for remote areas hereby and compared to with the literatures reported in the literature (Sami and Icaza, 2015).

Another study was proposed by for implementation in rural areas disconnected from the network. In addition, a photovoltaic and wind system designed for remote areas has been also suggested to supply uninterrupted power to a remote village in Chile by Covarrubias *et al.* (2005).



Figure-1. Wind turbine under investigation [<http://www.elmercurio.com.ec/342627-electricidad-domestica-con-la-fuerza-del-viento/>].

In addition, other studies were reported on PV-wind-battery hybrids and PV-wind-diesel-battery hybrids for rural electrification in Colombia (Howell *et al.*, 1982; Atideh and Zhenhua, 2008; Fargali *et al.*, 2010; Craig and Zhiwen, 2011; Mustafa, 2013; Saha *et al.*, 2013; Yoshimasa *et al.*, 2015). Furthermore, a numerical model based upon the energy conversion equations integrated and simultaneously solved to describe the total power generated by a hybrid solar photovoltaic, wind turbine and hydraulic turbine system was presented by Sami and Icaza (2015) where a simulation model was validated against experimental data. It is worthwhile noting that the energy conversion equations were coded with MATLAB-V13.2. In addition, reference (Sami and Icaza, 2015) presented an analysis of stability through the traces of the locus of the roots.

Puntahacienda is located in the Parish of Quingeo, Canton Cuenca, Province of Azuay, Ecuador, approximately 30 Km from the city of Cuenca going along Via El Valle passing through the localities of Santa Ana and La Libertad. Unfortunately this remote area is not connected to the grid. Therefore, the present model and analysis will be beneficial to this remote area.

This paper describes the simulation and validation of a combined wind and solar system for electric power generation with energy storage facilities. In addition, multivariable weather data including the wind speed and direction, the solar radiation, the rain fall and humidity as well as temperature were obtained using a weather

station installed at Puntahacienda- Quingeo. Moreover, the simulation model presented hereby includes modeling of battery, modern load controller and inverter.

### 1.1. Mathematical Modeling

The mathematical model is based upon the energy conversion equations and this simplified model that is a representative of the parameters of the mechanical and electrical systems under investigation that directly influence the power. The model uses the LaPlace formulation to carry out the simulations of the energy transformation equations of the electric energy and solar radiation (Spiegel, 1991; Whiteman, 2000; Katsuhiko, 2003; Garcia, 2006; Wenham, 2007; Marreno, 2011; Penyarat and Pascal, 2012; Akikur *et al.*, 2013; Dustin and Jack, 2014). This process allows us to find the best design option of the hybrid system. Figure. 2 presents the scheme used to study and simulation the energy formulation of the PV and wind turbine and can be used in the future for other types of renewable energy. However it should be pointed out that adjustments and calibrations must be made for integration of new types of renewable energy. In our case study, this model is intended for remote areas that are not connected to the grid.

### 1.2. Laplace Formulation

#### 1.2.1. General Block Diagram

The following describes the simulation model, energy conversion equations, and linear programming principles as well as the description of MATLAB block diagrams;

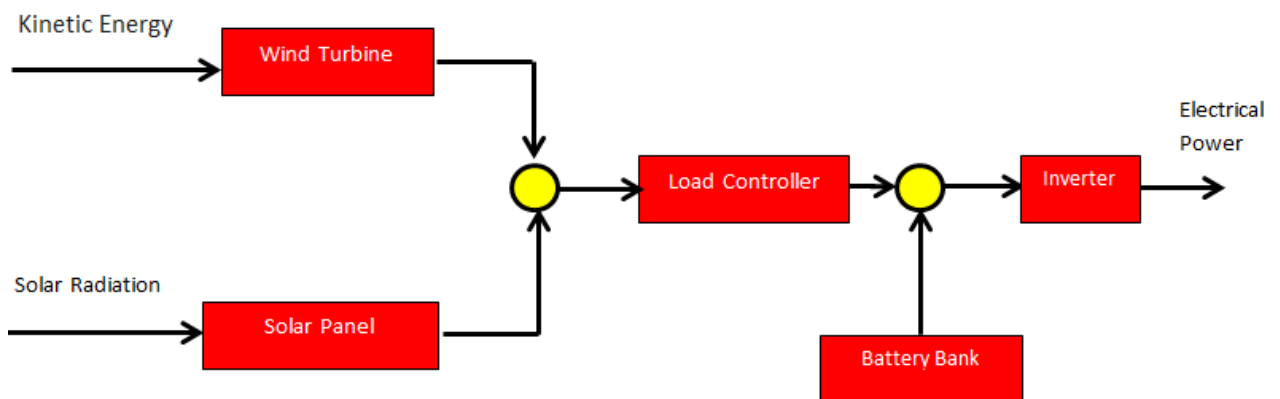


Figure-2. Electric Power Conversion Energy.

Figures 2 through (4) describe the block diagrams of the electric power conversion energy, the wind power generation as well as the direct current wind turbine formulations.

### 1.3. Block Diagram Wind Turbine

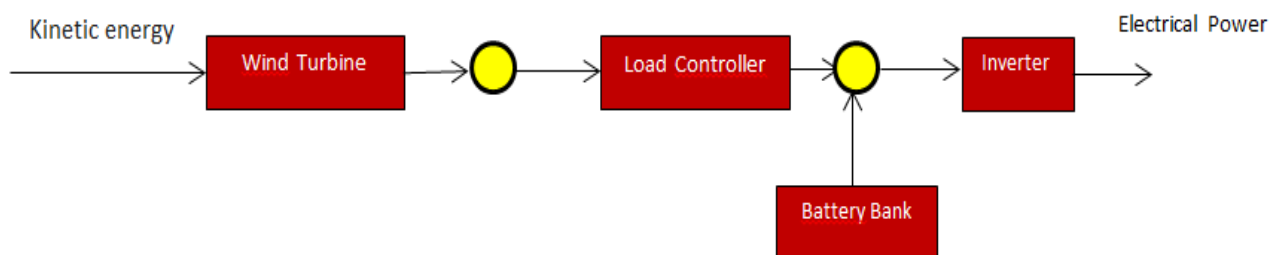


Figure-3. Block diagram of wind power generation.

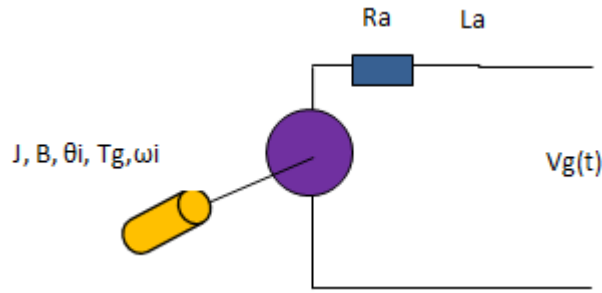


Figure-4. Simplified diagram of the direct current wind turbine.

Where the following define the nomenclatures used in these figures;

$K$  = Coefficient of proportionality of  $E_c$ .

$J$ = Moment of inertia at generator shaft.  $[[\text{Kg-m}^2]]$

$B$ = Viscous coefficient of friction of the generator.  $[[\text{N-m/rad/seg}]]$

$L_a$ = Armature Inductance  $[[\text{H}]]$

$R_a$ = Armature Resistance  $[[\Omega]]$

$\omega_i$ = Angular input speed (blades)

$\theta_i$ = Angular displacement of input (blades)

$T_g$ = Torque generator input (blades)

Furthermore, the following equations present the specific electrical parameters;

$$V_g(t) = R_a i_g + L_a \frac{di_g(t)}{dt} \Rightarrow \boxed{G_1}$$

$$V_g(s) = (R_a + L_a s) I_g(s) \tag{1}$$

However, the equations representing the mechanical parameters are as follows;

$$T_i(t) = B \omega_i(t) + J \frac{d\omega_i(t)}{dt} \Rightarrow \boxed{G_2}$$

$$T_i(s) = (B + Js) \omega_i(s) \tag{2}$$

And the generated electromotive force equations can be written as;

$$V_g(t) = K \omega_i(t) \Rightarrow \boxed{G_3}$$

$$V_g(s) = K \omega_i(s) \tag{3}$$

It is worthwhile pointing that the simplified block diagram shown in Figure.5 represents of the wind turbine according to equations (1), (2) and 3 in the Laplace domain;

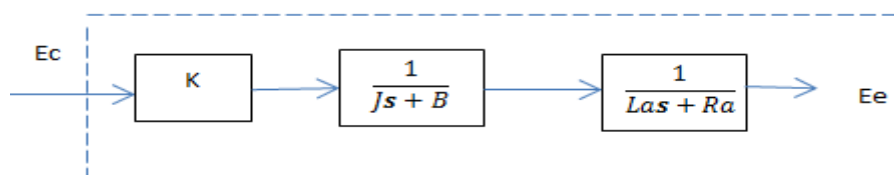


Figure-5. Block Diagram of the Wind Turbine.

Where; the following LaPlace domains are;

$$G_1(s) = \frac{1}{Ls + Ra}$$

$$G_2(s) = \frac{1}{Js + B}$$

$$G_3(s) = K$$

#### 1.4. Load Controller

The proportional industrial controller formula can be used to represent the load controller as shown in Figure.6;

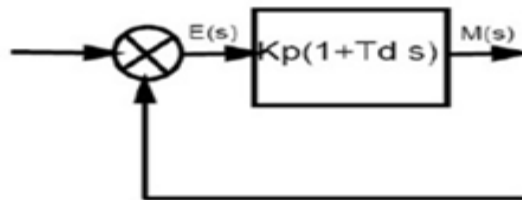


Figure-6. General diagram of the load controller.

Where parameters shown in Figure.6 are;

Kp= Proportional coefficient.

Td= Derivative time of the controller.

$$u(t) = Kp e(t) + Kp Td \frac{\delta e(t)}{\delta t} \quad (4)$$

$$\frac{U(s)}{E(s)} = Kp(1 + Td s) \quad (5)$$

Using equations (4) and (5) we obtain the Load Controller following relationship in the Laplace domain;

$$G_4(s) = Kp(1 + Td s) \quad (6)$$

#### 1.5. Inverter

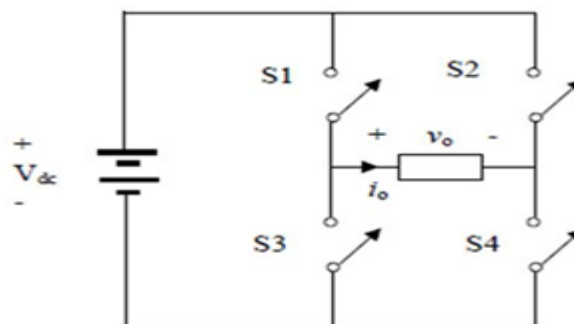


Figure-7. General diagram of the inverter.

The formulations describing the inverter in the time domain are presented as follows;

$$V_1(t) = K_3 V_3(t) \tag{7}$$

Transforming to the Laplace domain, we have:

$$V_1(s) = K_3 V_3(s) \tag{8}$$

Direct loop general diagram displays the wind generation system with operating parameters for the wind turbine as shown in Figure.8.

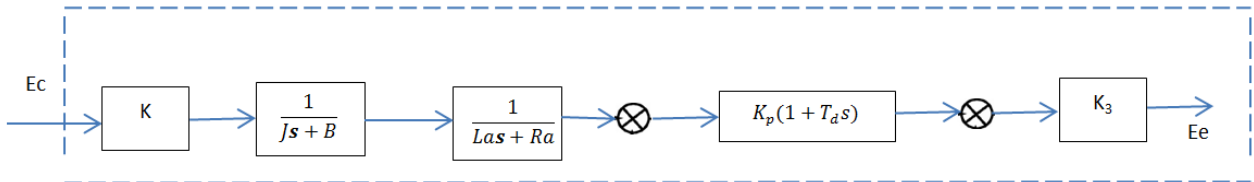


Figure-8. General diagram of the wind generation system with operating parameters.

Using the aforementioned block diagram and equations (9) through (11), we obtain the final transfer function of the input-output system in equation (12);

$$H(S) = K * \frac{1}{js+B} * \frac{1}{Las+Ra} * (Kp + KpTds) * K3 \tag{9}$$

$$H(s) = \frac{K*(Kp+KpTds)*K3}{(Js+B)(Las+Ra)} \tag{10}$$

$$H(s) = \frac{K*K3*Kp*Tds+K*Kp*K3}{JLa s^2+RaJs+BLas+RaB} \tag{11}$$

$$H(s) = \frac{K*K3*Kp*Tds+K*Kp*K3}{JLa s^2+(RaJ+BLa)s+RaB} \tag{12}$$

With the aforementioned transfer function, the system parameters can be evaluated.

### 1.6. Block Diagram Solar Panel

Figures (9) through (11) describe the block diagrams of the electric power conversion energy, the solar panel Photovoltaic PV power generation as well as the direct current solar PV formulations.

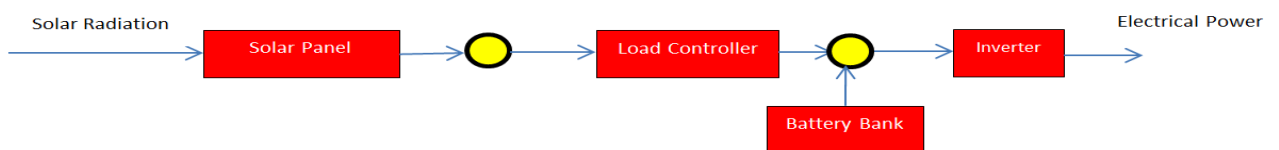


Figure-9. Diagram of the photovoltaic system.

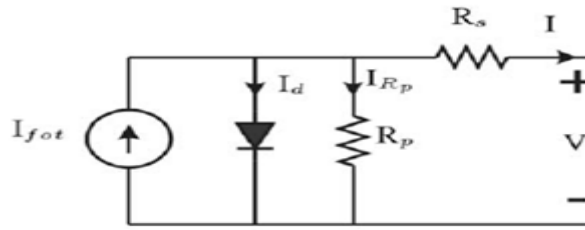


Figure-10. Diagram for the mathematical model for solar panel.

Solar panel PV collector current can be calculated as follows (Sami and Icaza, 2015; Sami and Icaza, 2015; Sami and Marin, 2017).

$$I_0 = I_g - I_{sat} \left\{ e^{\left( \frac{q(V_0 + I_0 R_s)}{AKT} \right)} - 1 \right\}$$

Where;

$q$  = Electron loading  $1.6 \cdot 10^{-19} C$

$K$  = Boltzmann's Constant

$A$  = Diode Factor

$T$  = Temperature of the cells.

$I_0$  = Initial current

$R_s$  = Resistance in series

$$\tau = \frac{V_0 + I_0 R_0}{AKT}$$

$$G_6(s) = \frac{1}{s + \tau}$$

The general diagram of the solar generation system with operating parameters is presented in Figure .11

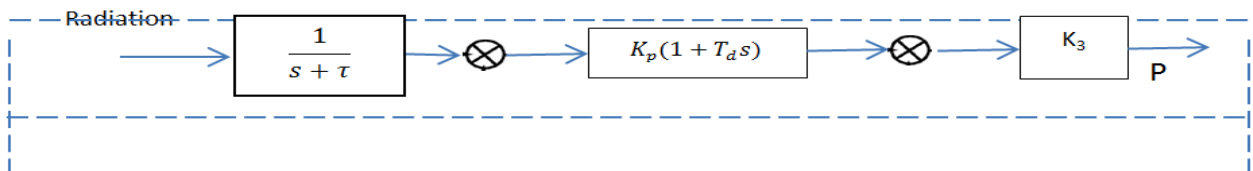


Figure-11. General diagram of the solar generation system with operating parameters.

Therefore, the transfer function can be written as follows;

$$H(s) = \frac{1}{s + \tau} * K_p(1 + T_d s) * K_3 \tag{13}$$

$$H(s) = \frac{K_p(1 + T_d s) * K_3 AKT}{AKT s + V_0 + I_0 R_0} \tag{14}$$

## 1.7. Energy Conversion Equations

### 1.7.1. Wind turbine Simulation

The power of a particular wind turbine is given by (Peterseim *et al.*, 2014; Sami and Icaza, 2015; Sami and Icaza, 2015).

$$P_{WT} = 0.5 * C_{p1} * \rho_{air} * A * v^3 * \eta_{aer} \quad (15)$$

Where;  $P_{WT}$  = Wind power sweep produced by the blades per unit area.  $C_{p1}$ = Betz power coefficient.

$\rho_{air}$ =Air density,  $A$  is the Area swept by the blades of the wind turbine and  $v$  is the wind velocity (Deissler, 1964; Covarrubias *et al.*, 2005).

Taking into account the internal performance of the wind turbine, the following can be written;

$$\eta_{aer} = \eta_{fmec} \cdot \eta_g \cdot \eta_{mp} \quad (16)$$

Where;  $\eta_{fmec}$ ,  $\eta_g$  are mechanical friction and generator efficiencies respectively and the efficiency speed multiplication box is  $\eta_{mp}$ .

The power output of the wind turbine can be expressed in single-phase power AC as;

$$P_{1f} = \sqrt{3} \cdot \eta_{c1} \cdot U_{line} \cdot I_{line} \cdot \cos\phi \quad (17)$$

With single phase AC power is  $P_{1f}$ , line current  $I_{line}$ , represents power factor  $\cos\phi$ , and the electric conversion efficiency is referred to as  $\eta_{c1}$ .

### 1.8. Efficiency of Photovoltaic PV System

The thermal energy absorbed by the PV solar collector is (Neira and Velecela, 2014; Peterseim *et al.*, 2014; Sami and Icaza, 2015; Sami and Icaza, 2015; Sami and Marin, 2017).

$$P_{pv} = \eta_{pvE} A_{pvE} G_t \quad (18)$$

Where  $\eta_{pvE}$  is PV solar collector efficiency,  $A_{pvE}$  is PV solar collector area (m<sup>2</sup>), and  $G_t$  is solar irradiation (W/m<sup>2</sup>) and  $\eta_{pvE}$  can be defined as Neira and Velecela (2014).

$$\eta_{pvE} = \eta_r \eta_{pc} [1 - \beta(T_c - T_{cref})] \quad (19)$$

Where  $\eta_{pc}$  is power conditioning efficiency which is equal to one when maximum power point tracking (MPPT) is used, and  $\beta$  is temperature coefficient ( (0.004 – 0.006) per °C), and  $\eta_r$  is the reference module efficiency, and  $T_{cref}$  is the collector reference temperature.

The characteristics performance "I-V" of the PV solar panel can be described by the following (Peterseim *et al.*, 2014; Srinivas and Reddy, 2014; Sami and Marin, 2017).

$$I = I_L(G_1, T_1) - N_p I_0 \left[ e^{\left( \frac{V + IR_s}{V_t} - 1 \right)} \right] - \frac{V + IR_s}{R_p} \quad (20)$$

$$V_t = mN_s k \frac{(T_1 + 273)}{qe} \quad (21)$$

$$I_0 = \frac{I_{sc} - \frac{V_{oc}}{R_p}}{e^{\left( \frac{V_{oc}}{V_t} \right)} - 1} \quad (22)$$

Where:

$N_s$  is the number of solar cells in series.

$N_p$  is the number of cells in parallel.

$k$  is the Boltzman constant.

$qe$  is the charge of the electron.

$m$  is the diode ideality factor;  $1 < m < 2$ .

$T_1$  is the working temperature of the solar panel in ° C.

$R_s$  is the series resistor.

$R_p$  is the resistance in parallel.

$I_L(G_1, T_1)$  is the photogenerated current and approximately equal to the short-circuit current  $I_{sc}(G_1, T_1)$ .

$I_0$  is the inverse saturation current of the diode.

$V_{oc}$  is the open circuit voltage (Fargali *et al.*, 2010; Sami and Marin, 2017).

The electric PV power output in DC taking into account the efficiency of conversion to electric energy is;

$$P_{PV}(t) = \eta_{c2} I_{PV}(t) \cdot V_{PV}(t) \quad (23)$$

Where  $\eta_{c2}$  is the efficiency of conversion to DC and referred to  $V_{PV}(t)$ , and  $I_{PV}(t)$ .

### 1.9. Controller

Generally, the controller power output is given by (Sami and Icaza, 2015; Sami and Marin, 2017).

$$P_{Cont-dc} = V_{bat} (I_{rect} + I_{PV}) \quad (24)$$

Where;  $V_{bat}$  is multiplication of the nominal voltage DC in the battery for any particular system and  $I_{rect}$  and

$I_{PV}$  represent the output current of the rectifier in DC and currents of PV.

### 1.10. Battery Charging and Discharging Model

The battery stores excess power going through the load charge controller (figure 12-a, and figure 12b). The battery also keeps voltage within the specified voltage and thus, protects over discharge rates, and prevent overload.

During the charging period, the voltage-current relationship can be described as follows (Marreno, 2011; Sami and Icaza, 2015; Sami and Icaza, 2015; Yoshimasa *et al.*, 2015; Sami and Marin, 2017).

$$V = V_r + \frac{I \left( \frac{0.189}{(1.142 - SOC) + R_i} \right)}{AH} + (SOC - 0.9) \ln \left( 300 \frac{I}{AH} + 1.0 \right) \quad (25)$$

And;

$$V_r = 2.094[1.0 - 0.001(T - 22^\circ C)] \quad (26)$$

However, during the discharging process and using equation (24), the current-voltage can be written as (Sami and Icaza, 2015; Sami and Marin, 2017);

$$V = V_r + \frac{I}{AH} \left( \frac{0.189}{SOC} + R_i \right) \quad (27)$$

And  $R_i$  is given by;

$$R_i(\Omega) = 0.15[1.0 - 0.02(T - 22^\circ C)] \quad (28)$$

Where,

$V_r$ , I: the terminal voltage and current respectively

$R_i(\Omega)$ : Internal resistance of the cell and  $T$  is the ambient temperature.

$AH$ : Ampere-hour rating of the battery during discharging process

Finally, the power produced by the PV array can be calculated by the following equation,

$$P = V I_{OUT_{rect}} \quad (29)$$

Where  $I_{OUT_{rect}}$  represent the total output current of the rectifier in DC (24).

### 1.11. Inverter

The characteristics of the inverter are given by the ratio of the input power to the inverter  $P_{inv-ip}$  and inverter output power  $P_{inv-op}$ . The inverter will incur conversion losses and to account for the inverter efficiency losses,  $\eta_{inv}$  is used (Sami and Icaza, 2015; Sami and Marin, 2017);

$$P_{inv-ip} \cdot \eta_{inv} = P_{inv-op} \quad (30)$$

The AC power of the inverter output  $P(t)$  is calculated using the inverter efficiency  $\eta_{inv}$ , output voltage between phases, neutral  $V_{fn}$ , for single-phase current  $I_o$  and  $\cos\phi$  as follows (Sami and Icaza, 2015; Sami and Marin, 2017);

$$P(t) = \sqrt{3} \eta_{inv} V_{fn} I_o \cos\phi \quad (31)$$

Finally, the hybrid system energy conversion efficiency for harnessing energy from wind turbine and PV is given by (Sami and Icaza, 2015; Sami and Marin, 2017);

$$\eta_{system} = \eta_{PV} * \eta_{wind} \quad (32)$$

$$\eta_{system} = \frac{P_{sf}}{P_{WT}+P_{PV}} \quad (33)$$

## 2. NUMERICAL PROCEDURE

The energy conversion and heat transfer mechanisms taking place during various processes shown in figure 12a and figure 12b, are described in Equations (15) through (33). These equations have been solved as per the logical flow diagram presented in Figure 13, to obtain the input parameters of wind and solar PV under different input conditions. Dependent parameters were calculated and integrated into the system of equations and solved numerically by convergence iterative method. Iterations were performed until a solution is reached with acceptable iteration error.

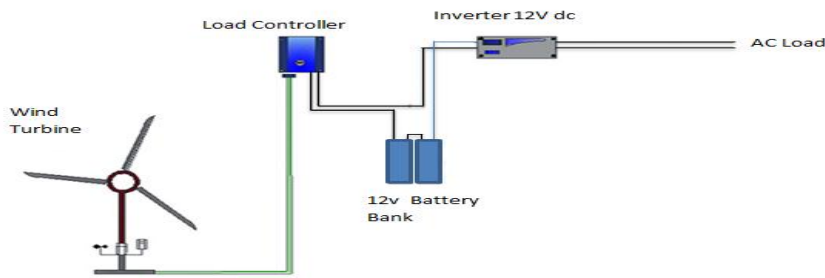


Figure-12-a. Wind subsystem

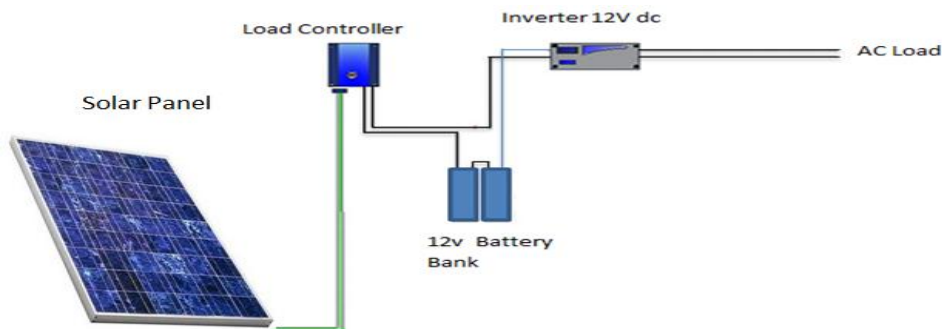


Figure-12-b. Solar subsystem.

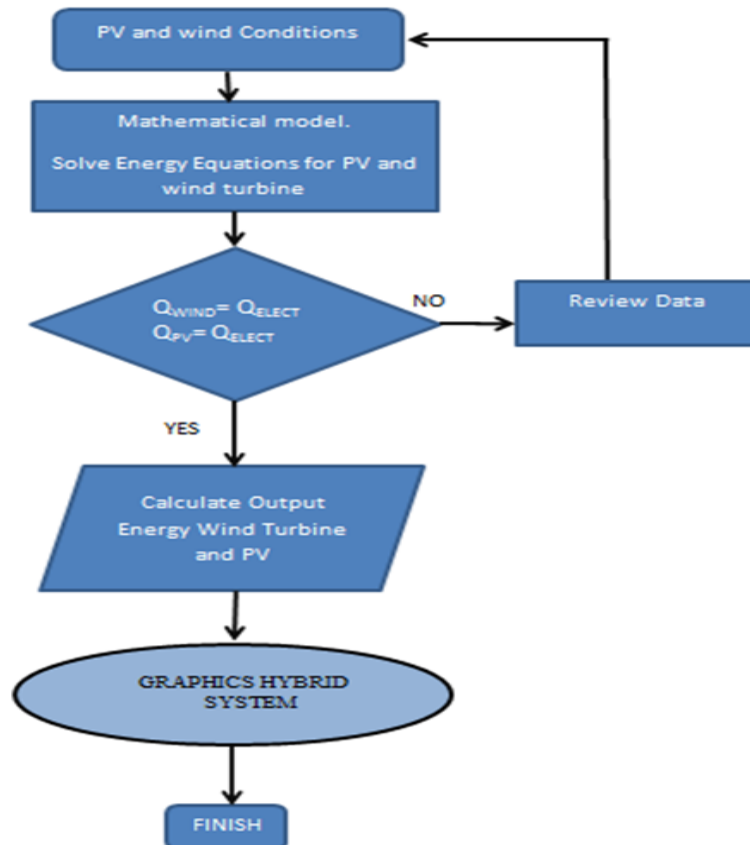


Figure-13. Flow diagram of Hybrid system calculation

### 3. RESULTS AND DISCUSSION

Equations (15) to (33) described earlier in this article were solved taking into account that the total power is not always be simultaneous, and for validation purposes, this simulation model and the equations were coded using MATLAB. In addition, in order to validate the model presented hereby and the simulated results were compared against literature data under various conditions. In the following sections, we present, analyze and discuss the predicted numerical results, as well as the validations of the simulation model in question.

In the Figure 14 through 16 the typical profiles of environmental parameters at the site during such as ambient temperature, solar radiation and wind speed are presented several the year 2016 at different times of the day. The environmental data presented in the aforementioned figures were used in the modeling and simulation of the system.

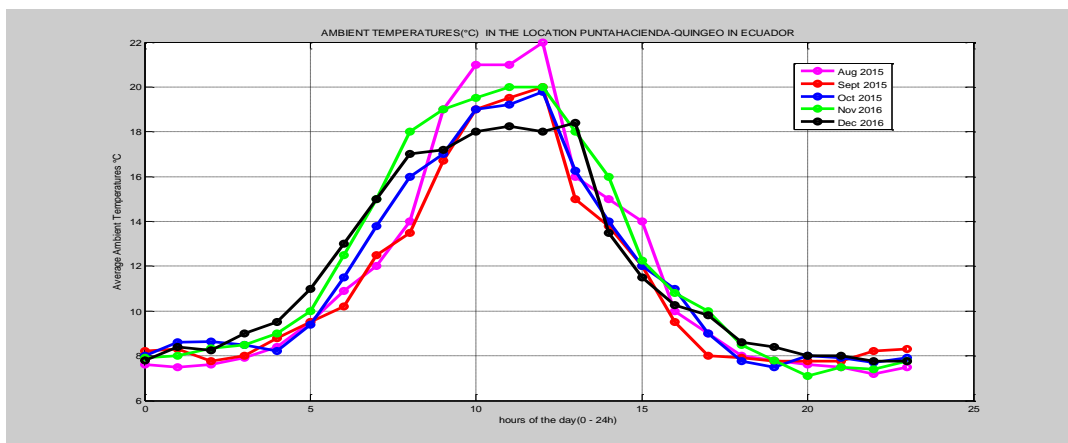


Figure-14. Ambient temperatures (°C) profile August 2016- December 2016

### 3.1. Wind Turbine Simulation

Figures 17 through 19 present the wind turbine simulation results where Betz Coefficient, wind turbine power and efficiency were displayed. In particular, the impact wind speed on the electrical power output generated by the wind turbine has been illustrated in Figures 17, 18 and 19. The predicted results displayed in these figures show that at the lower cut off speed of 2.5 m/s and higher cut off speed 9 m/s, the wind electrical power generated is 60 and 1900 Watts which coincide with the wind turbine specifications provided by the manufacturer (Sami and Icaza, 2015; Sami and Icaza, 2015). Furthermore, Figure 19 has been constructed to show the impact of the wind speed on the energy conversion efficiency from wind energy to electrical energy. It is quite clear that the higher wind speed results in higher energy conversion efficiency and produces more power output. However, for the wind turbine under investigation, the minimum starting wind speed is 2.5 m/s, at this particular condition, the power output and conversion efficiency are significantly low and economically viable.

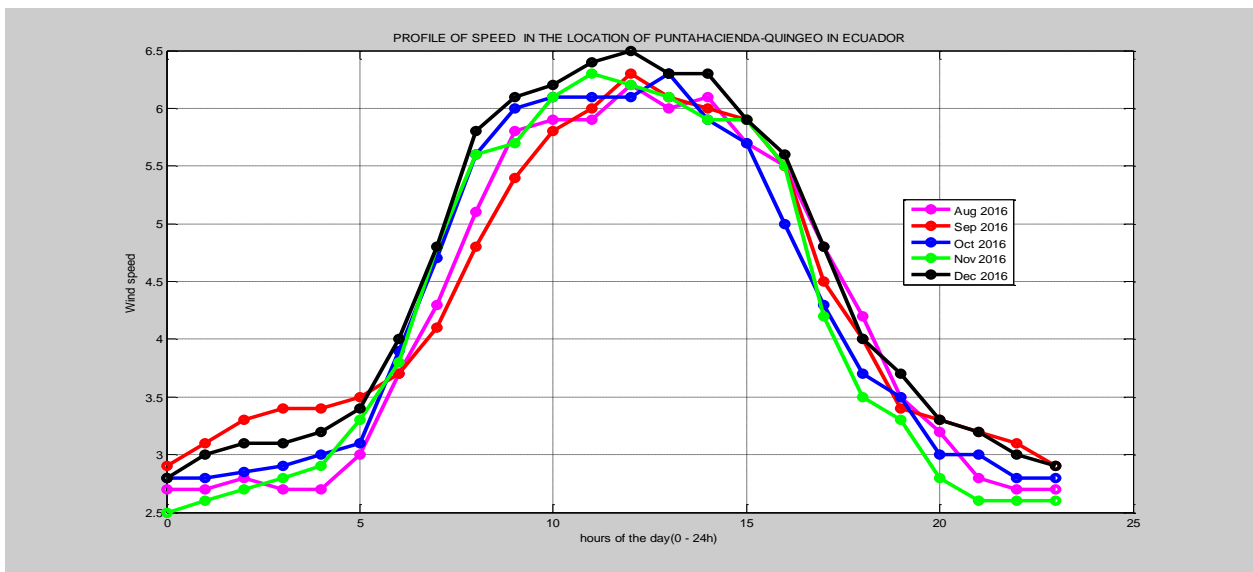


Figure-15. Profile of Speed in m/s Aug2016- Dec 2016

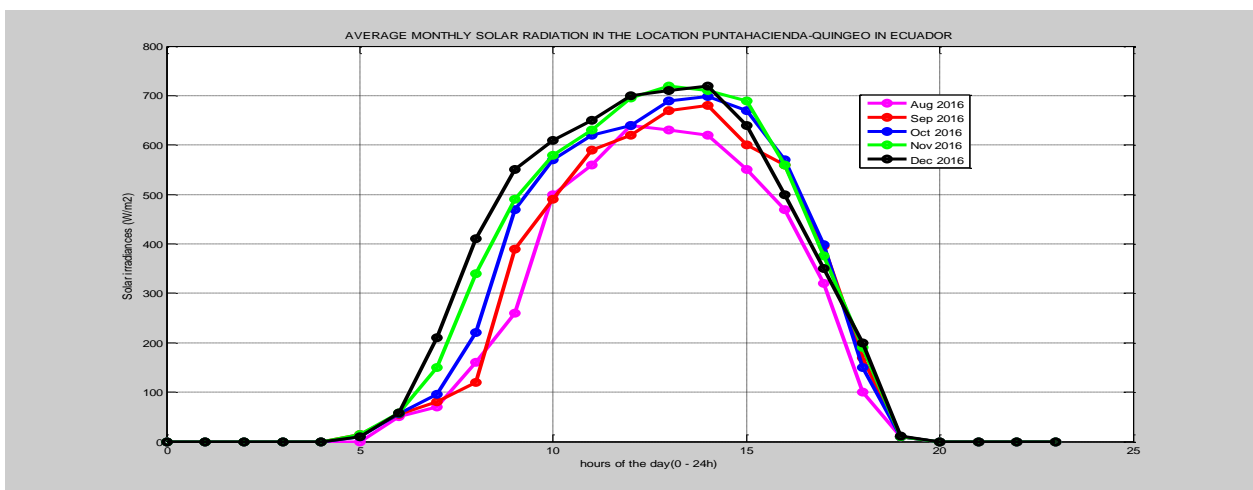


Figure-16. Solar irradiances (W/m<sup>2</sup>) Profile Aug 2016-Dec 2016

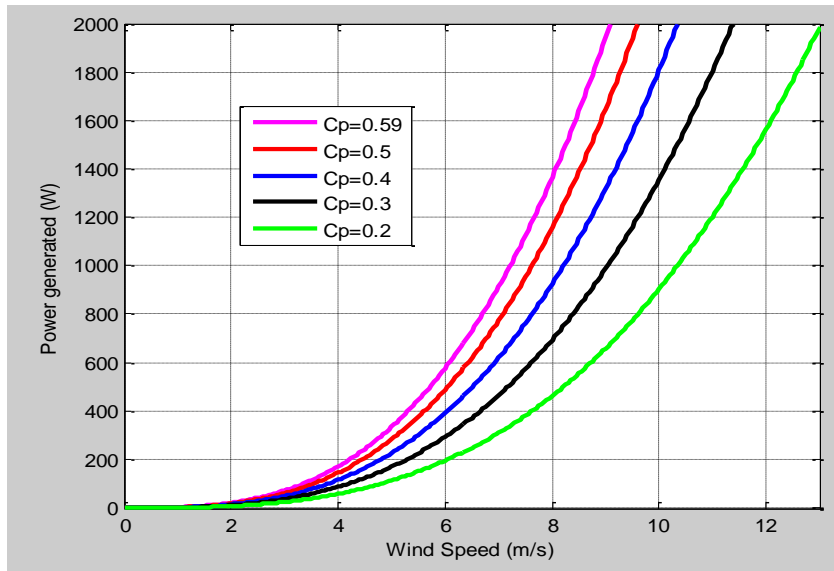


Figure-17. Power-speed curve for different values of Betz Coefficient.

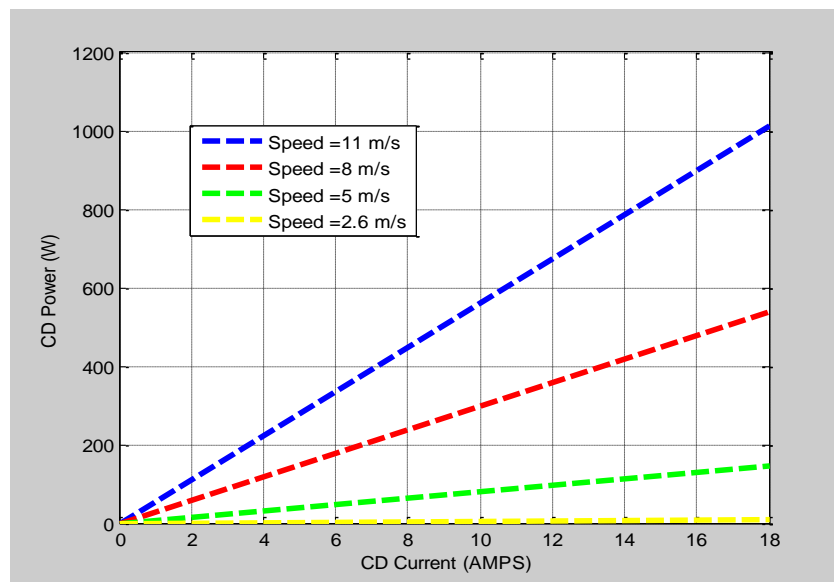


Figure-18. DC Power- DC Current for wind Speed (m/s).

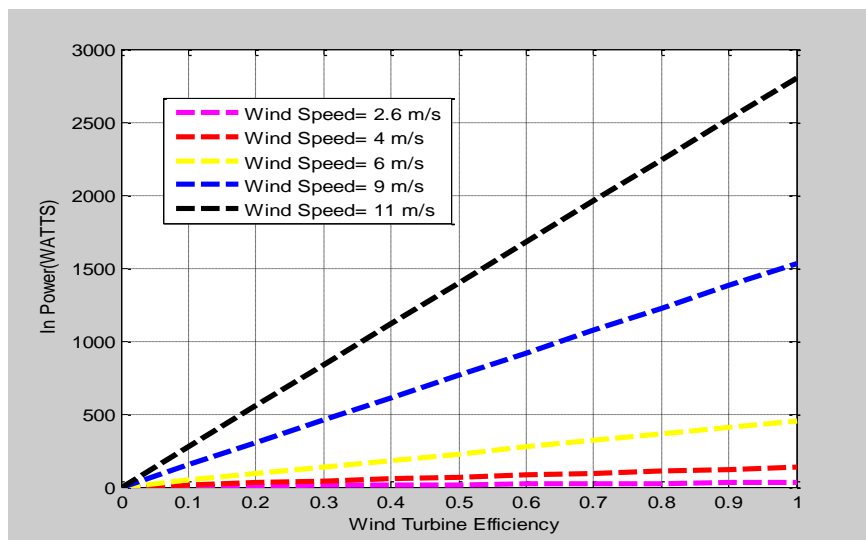


Figure-19. Energy conversion efficiency at various wind speeds

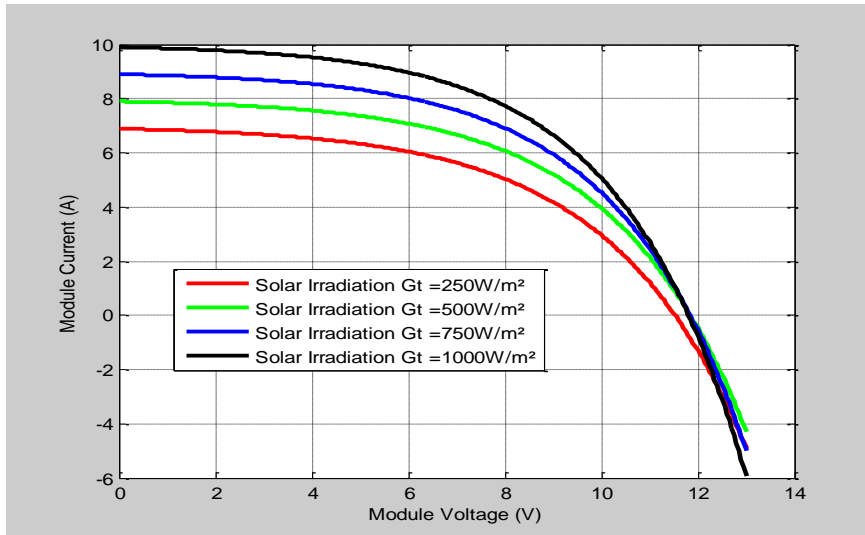


Figure-20. Voltage-Current curve for different values of irradiance-  $W/m^2$ .

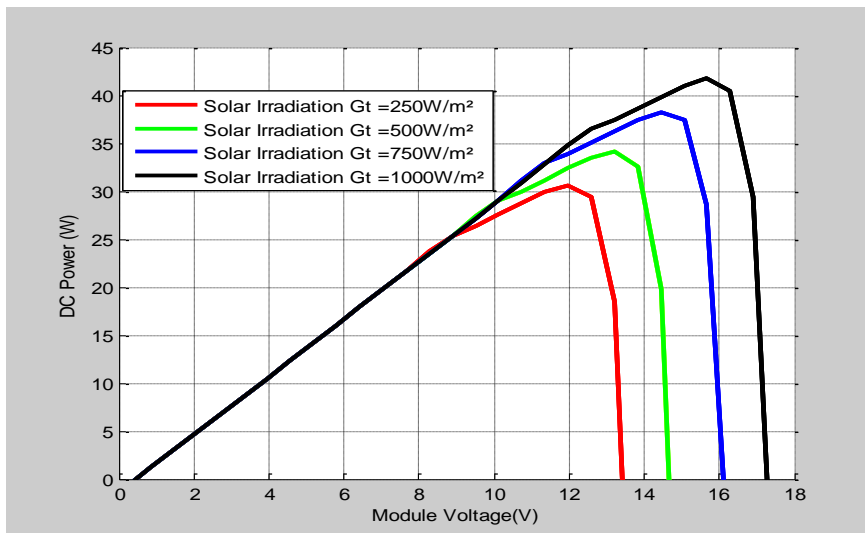


Figure-21. DC Voltage PV- DC Power PV for different values of irradiance ( $W/m^2$ ).

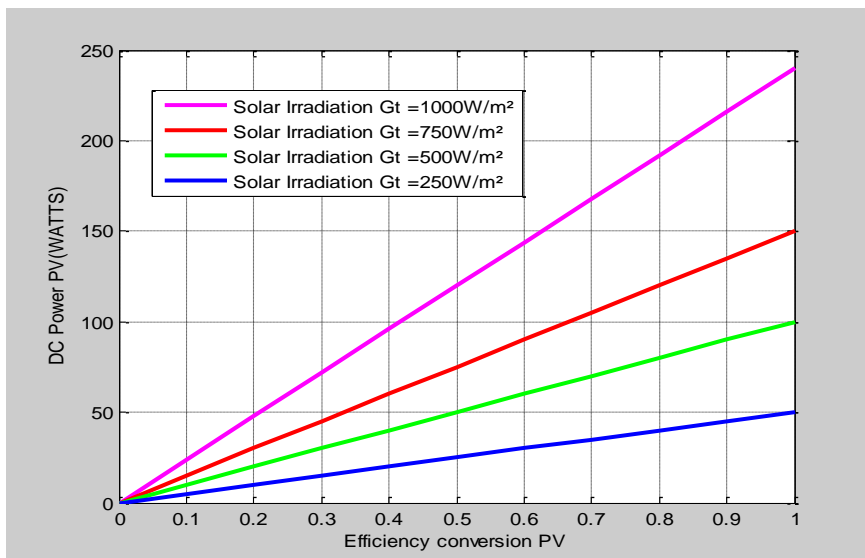


Figure-22. DC Power PV- Efficiency Conversion PV for different values of irradiance ( $W/m^2$ ).

### 3.2. PV Simulation

The PV characteristics such as voltage, amperage, output power and solar panel efficiency are displayed in Figures 20 through 22. In addition, these figures demonstrate the basic concept of energy conversion from the solar insolation into electrical energy as shown in particular in Figure 22. This figure shows the effect of solar radiation on the PV electrical power produced and energy conversion efficiency. It is worth noting that the numerical simulation presented hereby include the variation of PV cell temperatures from 10°C through 22°C (C.F. Figure.14). It is quite clear from figures 21 and 22 that higher solar radiation results in higher energy conversion efficiency and output PV electrical power. Therefore, it is quite evident that the solar panels will more efficient to operate at sites with higher solar irradiance (Sami and Icaza, 2015; Sami and Icaza, 2015; Sami and Marin, 2017).

On the other hand, using equation (31), the different possibilities of generation of electric energy in alternating current can be simulated and displayed in Figure.23. In this particular case, the values of  $\text{Cos } \phi = 0.9$ , system performance efficiency,  $\eta = 0.5$  and at different single phase AC current and considering the selected inverter, we can obtain in the single phase power in alternating current, as demonstrated in Figure 23.

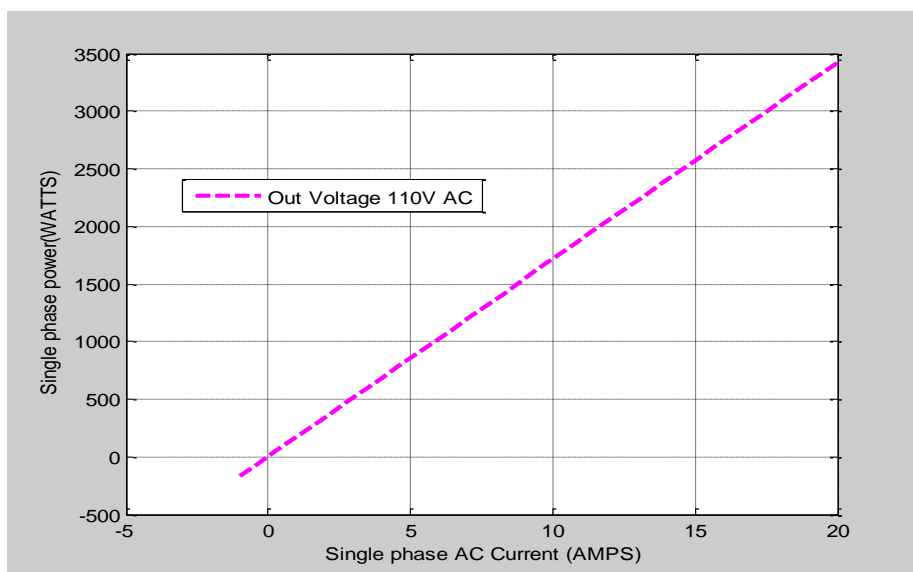


Figure-23. AC Current (A)– Electrical Power (W) for 110V,  $\text{Cos } \phi = 0.9$ .

### 3.3. Stability Analysis of the Hybrid System

The geometric root locus method (GRL) is very useful in designing a linear control system, since it describes how an open loop poles must be modified in order for meet the response and performance specifications of the system. This method is particularly convenient in obtaining approximate results very quickly.

Figures 24 and 25 were constructed after the transfer function described in equations (12) and (14), respectively for the wind and the PV systems, corresponding to the model is shown in Figure 8 and Figure 11. The input parameters are those generated in Figures 24 and 25 where the poles and zeros are located to determine if the status of the system is stable. In the case under investigation, it is stable because the poles are to the left with respect to the imaginary axis.

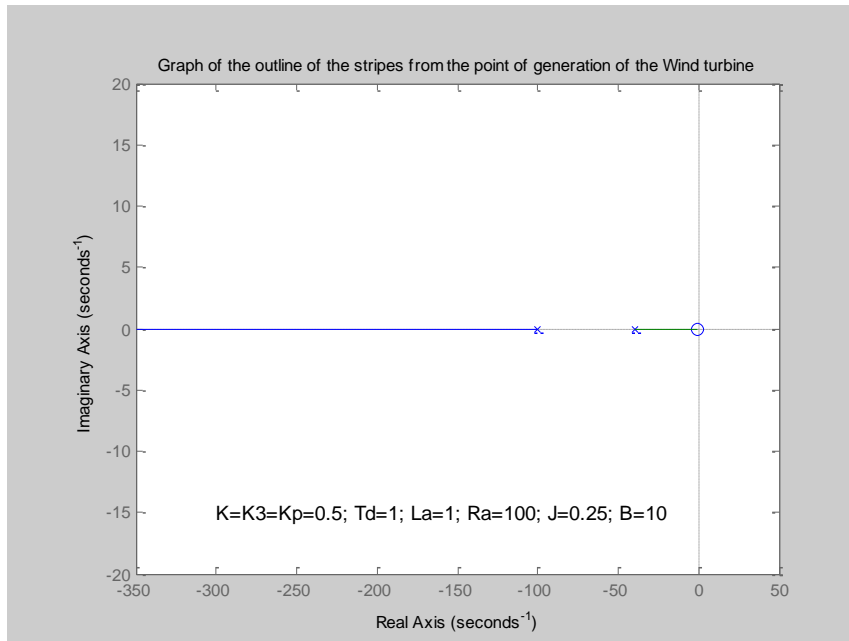


Figure-24. Graph of the geometric location of the roots referring to the wind turbine.

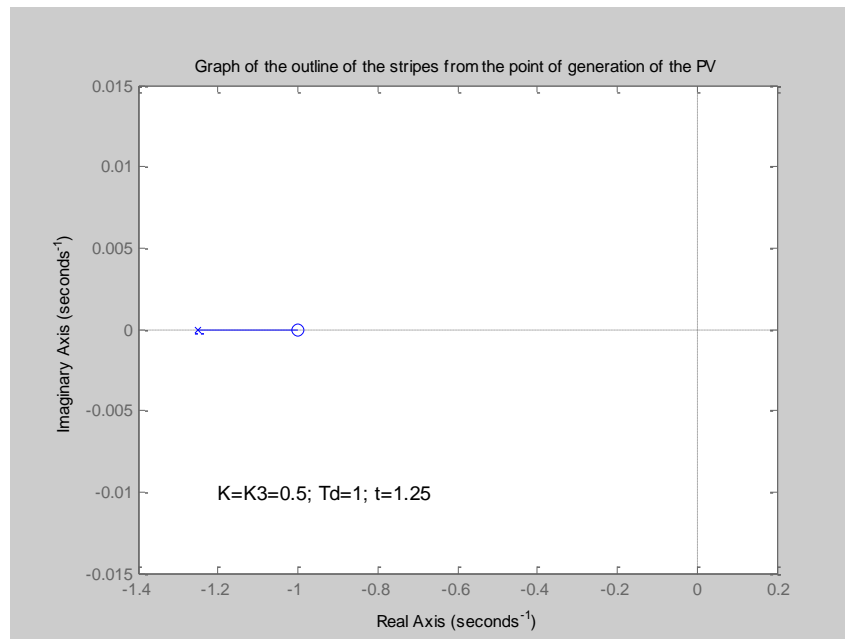


Figure-25. Graph of the geometric location of the roots referring to the PV.

### 3.4. Validation of the Simulation Model

In order to validate our numerical model prediction described in equations (15 through 33), the numerical results simulating the hybrid system in question were compared to data presented in reference (Fargali *et al.*, 2010; Sami and Icaza, 2015). To that end Figures 26, 27 and 28 have been constructed to present the model validation.

In Figure 26, we have presented the results from the mathematical model used simulated in Matlab and compared to the power data measured at different wind velocities (Sami and Icaza, 2015). The discrepancy between the model and the simulated data can be attributed to the fact that the Betz coefficient considered in the modeling was the optimum value;  $C_p = 0.59$ , and the data available were at approximately using  $C_o=0.46$ .

The numerical results predicted by the model in Matlab and compared well to the measurements (Fargali *et al.*, 2010) for voltages higher than 7 V in Figure .27. However, lower current were predicted at voltages under 7 V.

A comparison between the results of the Matlab model and solar panel data is presented in (Kavitha and Kamdi, 2013; Sami and Icaza, 2015) in Figure. 28. It can be observed from this figure that solar panel power increases as a function of the generated voltage up to a certain limit of 14 V and then significantly power is reduced

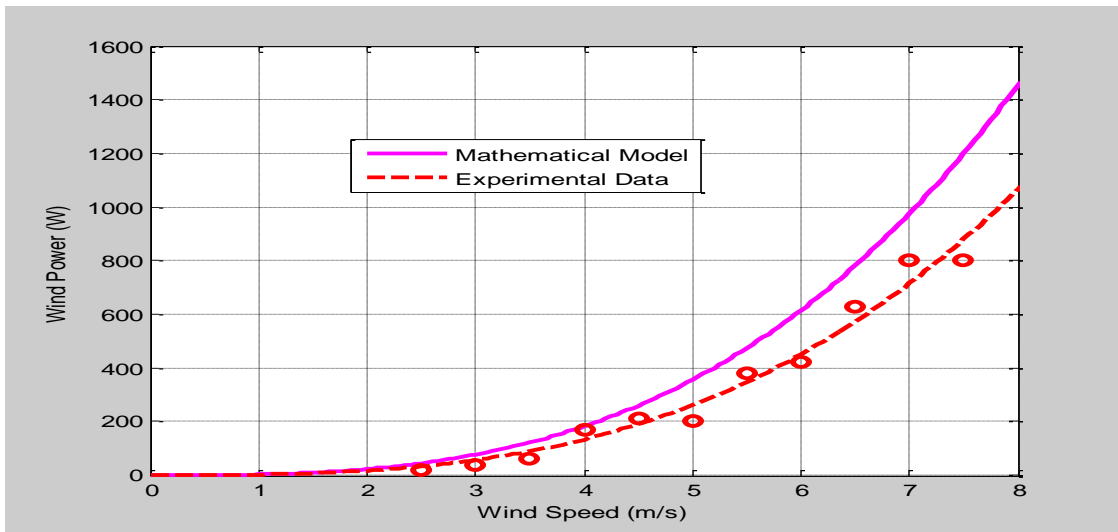


Figure-26. Comparison of Wind speed – Wind Power (Sami and Icaza, 2015).

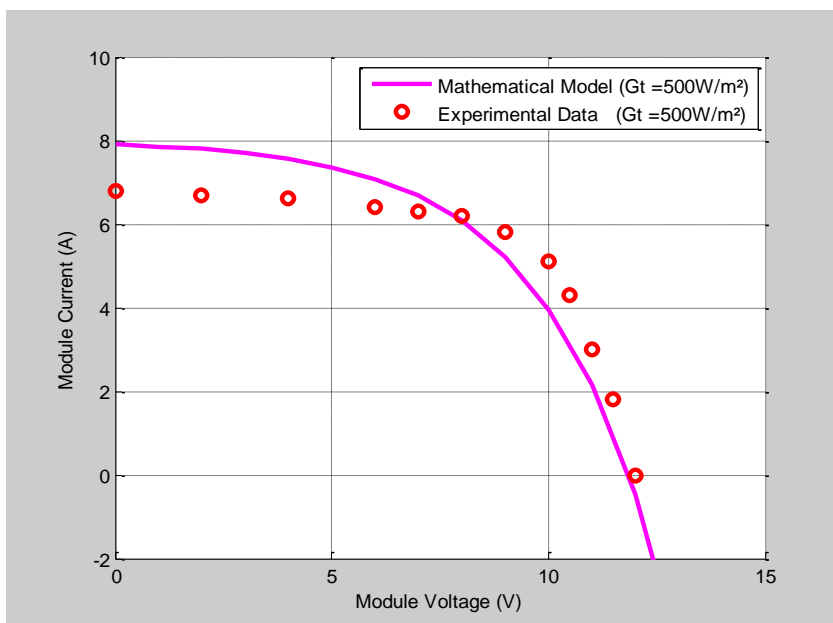


Figure-27. PV output data (Fargali *et al.*, 2010) compared to model prediction at 500 W/m<sup>2</sup>.

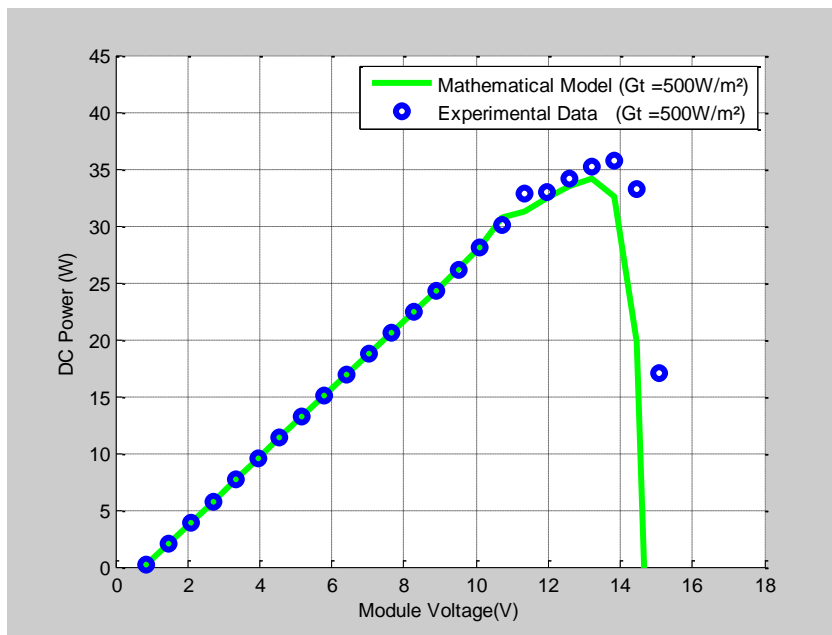


Figure-28. PV output data compared to model prediction at 500 W/m<sup>2</sup> (Kavitha and Kamdi, 2013; Sami and Icaza, 2015).

#### 4. CONCLUSIONS

The modeling, simulation and analysis of the energy conversion equations describing the behavior of a hybrid system PV and wind turbine, and hybrid system for electrical power generation are presented. A numerical model based on the aforementioned equations was developed; coded using MATLAB and results were presented, discussed and compared to experimental data reported in the literature. The model prediction compared fairly with the PV data at different conditions.

A stability analysis was also performed by the mathematical modeling for the hybrid system. It is important to point out that this analysis has been carried out so that in the near future one of these power generation systems to be exploited to a great extent in the locality of Quingeo-Puntahacienda, It is concluded that the present system can be considered for Quingeo-Puntahacienda as a renewable energy system and it is favorable.

##### 4.1. Nomenclature

$A_{pve}$ : PV solar collector area (m<sup>2</sup>)

$B$ : Device and material constant

$\cos\phi$ : Power factor referred to wind turbine.

$C_{p1}$ : Betz power coefficient.

$E_g$ : Stefan Boltzmann Coefficient

$E_{g0}$ : Band gap Energy at 0° K

$G_t$ : Solar irradiation (W/m<sup>2</sup>)

$H1$ : Altitude difference.

$I_0$ : Reverse saturation current and is a function of the cell temperature.

$I_L$ : Load current

$I_{line}$ : Line current referred to wind turbine.

$I_{rect}$ : DC current to the rectifier output.

LLP: Loss of load probability.

$P(t)$ : AC power of the inverter output.

$P_{1f}$ : Single phase AC power of the wind turbine.

$P_{pv}$ : Nominal Power PV.

$P_{PV}(t)$ : Electrical power DC of PV.

$P_{WT}$ : Wind power sweep produced by the blades.

$P_{Cont-dc}$ : Power Controller.

$P_{inv-ip}$ : Inverter input power.

$P_{inv-op}$ : Inverter output power.

$Q_{in}$ : Solar energy absorbed by the module

$Q_{elect}$ : Electric power produced

$T_C$ : The cell temperature (K)

$T_r$ : Reference temperature (K)

$\Delta T$ : Temperature difference ( $T_c - T_a$ )

$(T_C - T_r)$ : Difference between reference temperature (298 K) and cell temperature.

$v$ : Wind speed

$V_{PV}(t)$ : Voltage referred to PV in DC.

$U_{line}$ : Line voltage referred to wind turbine.

V: The output voltage of the PV array and approximately equal to the battery voltage.

$V_{fn}$  : Phase- neutral voltage.

$V_{bat}$ : Nominal voltage DC in the battery.

$N_{SBat}$ : Number of batteries connected in series.

#### 4.2. Greek alphabet

$\alpha_{abs}$  : Overall absorption coefficient

$\beta$ : Tilt angle

$\rho_{air}$ = Air density.

$\eta_{aer}$  : Wind turbine efficiency.

$\eta_{mec}$  : Mechanical friction efficiency.

$\eta_g$ : Generator machine efficiency.

$\eta_{mp}$ : Speed multiplication box efficiency.

$\eta_{c1}$ : Electric conversion efficiency is referred to wind turbine.

$\eta_{pv\#}$  : PV solar collector efficiency.

$\eta_r$  : The reference module efficiency

$\eta_{c2}$ : The efficiency of conversion to DC referred to PV

$\eta_{pc}$  : Power conditioning efficiency

$\eta_{inv}$ : Inverter efficiency.

$\eta_{system}$ : Hybrid system efficiency.

$\eta_o$ : Module efficiency at reference temperature (298 K)

$\eta_{inv}$ = Inverter efficiency

#### 4.3. Subscripts

aer - Aero generator

Air – Air

*bat* – Battery

*Cont – dc* Controller

*c1* – Electric conversion referred to wind turbine.

*c2* – Conversion to DC referred to PV

*fn* – Phase neutral

*inv – ip* - Inverter input

*inv – op* - Inverter output

p – Power

*pc* – Power conditioning

PV – Photo Voltaic

pvg – Irradiance PV

rect – Rectifier

*SBat* – Batteries connected in series.

*total* – Total

*1f* – Single phase AC

**Funding:** The research work presented in this paper was made possible through the support of the Catholic University of Cuenca.

**Competing Interests:** The authors declare that they have no competing interests.

**Contributors/Acknowledgement:** The research work presented in this paper was also made possible in part by the support of Daniel Icaza's family who helped to move the equipment to where the tests were carried out. The co-author Daniel Icaza acknowledges the support of Professor Dr. Samuel Sami Howard who forged him as a researcher at the Research Center for Renewable Energy, CER, when he started to work at the Catholic University of Cuenca.

## REFERENCES

- Akikur, R.K., R. Saidur, H. Ping and K.R. Ullah, 2013. Comparative study of stand-alone and hybrid solar energy systems suitable for off-grid rural electrification: A review. *Renewable and Sustainable Energy Reviews*, 27: 738-752. [View at Google Scholar](#) | [View at Publisher](#)
- Atideh, A. and J. Zhenhua, 2008. Design and analysis of a fuel cell/gas turbine hybrid power system. Power and Energy Society General Meeting - Conversion and Delivery of Electrical Energy in the 21st Century, 2008 IEEE.
- Binayak, B., R.P. Shiva, L. Kyung-Tae and A. Sung-Hoon, 2014. Mathematical modeling of hybrid renewable energy system: A review on small hydro-solar-wind power generation. *International Journal of Precision Engineering and Manufacturing-Green Technology*, 1(2): 157-173. [View at Google Scholar](#) | [View at Publisher](#)

- Castillo, A., F. Villada and J.A. Valencia, 2014. Multiobjective design of a wind-solar hybrid system with batteries for non-interconnected areas. *University of Antioquia, Tecnura*, 18(39): 77-93.
- Covarrubias, F., I. Irrarrázaval and R. Galáz, 2005. Challenges of rural electrification in Chile. Washington, D.C. 20433, USA.
- Craig, T.S. and M. Zhiwen, 2011. Gas turbine/solar parabolic trough hybrid designs. To be presented at the ASME Turbo Expo 2011, Vancouver, Canada, June 6-10, 2011.
- Deissler, G., 1964. Diffusion approximation for thermal radiation in gases with jump boundary conditions. *Journal of Heat Transfer*, 86(2): 240-246. [View at Google Scholar](#) | [View at Publisher](#)
- Department of Energy, 2007. Potential benefits of distributed generation and rate related issues that may impede their expansion, a study pursuant to section 1817 of the energy policy act of 2005. February 2007. U.S. Department of Energy.
- Dustin, M. and B. Jack, 2014. Scott Samuelsen, fuel cell-gas turbine hybrid system design part I: Steady state performance. *Journal of Power Sources*, 257: 412-420.
- Fargali, H. M., F.H. Fahmy and M.A. Hassan, 2010. A simulation model for predicting the performance of PV/wind- powered geothermal space heating system in Egypt. *Online Journal on Electronics and Electrical Engineering*, 2(2): 321-330. [View at Google Scholar](#)
- Garcia, M., 2006. Modelado de sistemas fotovoltaicos autónomos. En: *Fundamentos, dimensionado y aplicaciones de la energía solar fotovoltaica*. Madrid: Centro de Investigaciones Energéticas, Medioambientales y Tecnológicas (CIEMAT). pp: 13.
- Howell, J.R., R.B. Bannerot and G.C. Vliet, 1982. *Solar-thermal energy systems: Analysis and design*. New York: McGraw-Hill, Inc.
- Iftekhhar, H.C.M., A. Duffy and B. Norton, 2015. A comparative technological review of hybrid CSP-biomass CHP systems in Europe. *International Conference on Sustainable Energy & Environmental Protection*, Paisley, UK, 11-14 August.
- Katsuhiko, O., 2003. *Modern control engineering*. 4th Edn., Madrid: Pearson, Prentice Hall. pp: 965.
- Kavitha, S. and S.Y. Kamdi, 2013. Solar hydro hybrid energy system simulation. *International Journal of Soft Computing and Engineering*, 2(6): 500-503.
- Marreno, S.M., 2011. Parameters of roughness representative of natural terrains. Thesis for Master's Degree in Geophysics and Meteorology, Department of Applied Physics, University of Granada, Granada, Spain: University of Granada.
- Mustafa, E., 2013. Sizing and simulation of PV-wind hybrid power system. *International Journal of Photoenergy*: 1-10. [View at Google Scholar](#) | [View at Publisher](#)
- Neira, R. and M. Velecela, 2014. Feasibility study of electricity generation using wind energy and photovoltaic solar energy for the Garauzhi sector of the Quingeo Parish belonging to the City of Cuenca. Ecuador: UPS.
- Penyarat, C. and B. Pascal, 2012. The hybrid solid oxide fuel cell (SOFC) and gas turbine (GT) systems steady state modeling. *International Journal of Hydrogen Energy*, 37(11): 9237-9248. [View at Google Scholar](#) | [View at Publisher](#)
- Peterseim, J.H., U. Hellwig, A. Tadros and S. White, 2014. Hybridisation optimization of concentrating solar thermal and biomass power generation facilities. *Science Direct Solar Energy*, 99: 203- 214. [View at Google Scholar](#) | [View at Publisher](#)
- Saha, N.C., S. Acharjee, M.A.S. Mollah, K.T. Rahman and F.H.M. Rafi, 2013. Modeling and performance analysis of a hybrid power system. *Proc. of International Conference on Informatics Electronics & Vision (ICIEV)*. pp: 1-5.
- Sami, S. and D. Icaza, 2015. Modeling, simulation of hybrid solar photovoltaic, wind turbine and hydraulic power system. *International Journal of Engineering Science and Technology*, 7(9): 304-317. [View at Google Scholar](#)
- Sami, S. and D. Icaza, 2015. Numerical modeling, simulation and validation of hybrid solar photovoltaic, wind turbine and fuel cell power system. *Journal of Technology Innovations in Renewable Energy*, 4(3): 96-112. [View at Google Scholar](#) | [View at Publisher](#)
- Sami, S. and E. Marin, 2017. Simulation of solar photovoltaic, biomass gas turbine and district heating hybrid system. *International Journal of Sustainable Energy and Environmental Research*, 6(1): 9-26. [View at Google Scholar](#) | [View at Publisher](#)
- Spiegel, M.R., 1991. *Laplace transforms*. 1st Edn., Mexico: McGraw-Hill. pp: 261.

- Srinivas, T. and B.V. Reddy, 2014. Hybrid solar -biomass power plant without energy storage. Reference: CSITE22, Appeared in: Case Studies in Thermal Engineering.
- Wenham, S., 2007. Applied photovoltaics. 2nd Edn., London: Earthscan. pp: 134.
- Whiteman, C.D., 2000. Mountain meteorology: Fundamentals and applications. Oxford: Oxford University Press.
- Yoshimasa, A., O. Hiroyuki, M. Masahiro, I. Hirroki, U. Yasutaka and I. Takuo, 2015. Demonstration of SOFC-micro gas turbine (MGT). Mitsubishi Heavy Industries Technical Review, 52(4): 47-52. [View at Google Scholar](#)
- Zhang, H.L., J. Baeyens, J. Degreve and G. Caceres, 2013. Concentrated solar power plants: Review and design methodology. Renewable and Sustainable Energy Reviews, 22: 466-481. [View at Google Scholar](#) | [View at Publisher](#)

## BIBLIOGRAPHY

<http://www.elmercurio.com.ec/342627-electricidad-domestica-con-la-fuerza-del-viento/>

*Views and opinions expressed in this article are the views and opinions of the author(s), International Journal of Management and Sustainability shall not be responsible or answerable for any loss, damage or liability etc. caused in relation to/arising out of the use of the content.*